

## Dominant Circulation Patterns of the Deep Gulf of Mexico

PAULA PÉREZ-BRUNIUS

*Department of Physical Oceanography, Centro de Investigación Científica y de Educación Superior de Ensenada, Baja California, Mexico*

HEATHER FUREY AND AMY BOWER

*Department of Physical Oceanography, Woods Hole Oceanographic Institution, Woods Hole, Massachusetts*

PETER HAMILTON

*Leidos Corporation, Raleigh, North Carolina*

JULIO CANDELA AND PAULA GARCÍA-CARRILLO

*Department of Physical Oceanography, Centro de Investigación Científica y de Educación Superior de Ensenada, Baja California, Mexico*

ROBERT LEBEN

*Colorado Center for Astrodynamics Research, University of Colorado Boulder, Boulder, Colorado*

(Manuscript received 13 July 2017, in final form 15 December 2017)

### ABSTRACT

The large-scale circulation of the bottom layer of the Gulf of Mexico is analyzed, with special attention to the historically least studied western basin. The analysis is based on 4 years of data collected by 158 subsurface floats parked at 1500 and 2500 m and is complemented with data collected by current meter moorings in the western basin during the same period. Three main circulation patterns stand out: a cyclonic boundary current, a cyclonic gyre in the abyssal plain, and the very high eddy kinetic energy observed in the eastern Gulf. The boundary current and the cyclonic gyre appear as distinct features, which interact in the western tip of the Yucatan shelf. The persistence and continuity of the boundary current is addressed. Although high variability is observed, the boundary flow serves as a pathway for water to travel around the western basin in approximately 2 years. An interesting discovery is the separation of the boundary current over the northwestern slope of the Yucatan shelf. The separation and retroflection of the along-slope current appears to be a persistent feature and is associated with anticyclonic eddies whose genesis mechanism remains to be understood. As the boundary flow separates, it feeds into the westward flow of the deep cyclonic gyre. The location of this gyre—named the Sigsbee Abyssal Gyre—coincides with closed geostrophic contours, so eddy–topography interaction via bottom form stresses may drive this mean flow. The contribution to the cyclonic vorticity of the gyre by modons traveling under Loop Current eddies is discussed.

### 1. Introduction

The Gulf of Mexico (GOM) is a highly stratified basin whose dynamics largely follow those of a two-layer system. The upper layer (above 800–1000 m) is characterized by surface-intensified flows, while the lower

layer (>1200 m to the bottom) shows currents that do not vary with depth (e.g., [Hamilton 2009](#)). The upper-layer circulation is dominated by the Loop Current (LC) and its associated eddies. The LC is part of the western boundary current of the North Atlantic subtropical gyre (e.g., [Candela et al. 2002](#)). It enters the GOM through the Yucatan Channel and exits via the Straits of Florida, turning clockwise in a meander that expands and contracts in the eastern basin (e.g., [Oey et al. 2005](#)).

The LC sheds large (~200–300 km) and energetic anticyclones at irregular intervals that are typically

---

 Denotes content that is immediately available upon publication as open access.

---

*Corresponding author:* Paula Pérez-Brunius, [brunius@cicese.mx](mailto:brunius@cicese.mx)

between 4 and 12 months but in some instances can be 18 months or longer in duration (Leben 2005; Hall and Leben 2016). After separation from the LC, these eddies travel westward until they dissipate due to processes not yet fully understood, which involve vertical mixing induced by air–sea fluxes and enhanced submesoscale activity around the rings' periphery, and interactions with other mesoscale structures and with the western boundary (e.g., Biggs et al. 1996; Hamilton 2002; Vidal et al. 1992, 1994; LaCasce 1998; Mahadevan et al. 2008).

In the southern GOM, a semipermanent cyclonic circulation—the Campeche Gyre—is found in the upper layer, which has been suggested is an equivalent barotropic flow, hence extending to the lower layer (Pérez-Brunius et al. 2013). The gyre was observed at 900 m in the PALACE floats study by Weatherly et al. (2005), but the lack of observations below 1000 m has not made it possible to confirm if it extends to the deep layer.

The circulation of the deep GOM waters is less well known, although several studies indicate that the LC and mesoscale eddies greatly influence the dynamics of the bottom layer. The deep eastern GOM has been explored more, thanks to several observational programs and modeling studies (e.g., Donohue et al. 2016; Hamilton et al. 2016a; Lee 2003; Oey 2008; Oey and Lee 2002; Sheinbaum et al. 2016). These studies show that the main source of energy in the deep eastern basin comes from the expansion and retraction of the Loop Current, which induces movement in the lower layer via baroclinic instabilities, deep eddies, and topographic Rossby waves (TRWs) that can transfer energy toward the western basin, both to the interior and along the northern boundary.

Numerical studies suggest the presence of a mean cyclonic flow around the deep basin (e.g., Bracco et al. 2016; Hurlburt and Thompson 1980; Lee 2003; Oey and Lee 2002), and hydrographic data analyzed with inverse techniques or in combination with PALACE floats parked at 900 m show evidence suggesting this is the case (Hofmann and Worley 1986; DeHaan and Sturges 2005). More recently, an array of deep-water moorings in the western and southern Gulf of Mexico sustain this claim (Tenreiro et al. 2018). Along the continental slope, current meter moorings and subsurface floats have confirmed the existence of a mean westward flow over the northern slope (e.g., Donohue et al. 2006; Hamilton 2009). The mooring observations of Tenreiro et al. (2018) also show mean flow along the western boundary, although it is less clear if this flow continues into the Bay of Campeche (BOC). Hence, the presence, continuity, and persistence of the boundary current all around the Gulf of Mexico remain unknown.

The forcing for the deep boundary current has been typically attributed to rectification of TRWs (e.g.,

DeHaan and Sturges 2005; Hamilton 1990; 2009; Oey and Lee 2002; Mizuta and Hogg 2004). TRWs with periods ranging between 20 and 100 days have been observed over the northern slope, generated by the complex interaction between the upper and lower layers resulting from the dynamics of the Loop Current and the detachment of Loop Current eddies in the northeastern Gulf (e.g., Donohue et al. 2006; Hamilton 1990; Hamilton et al. 2016a; Hamilton and Lugo Fernandez 2001; Lee 2003; Oey and Lee 2002).

In the northwestern Gulf, LC rings that interact with the slope may also generate TRWs (Oey and Lee 2002; Hamilton 2009), although moorings on the northern part of the western slope (Rio Grande slope) show no evidence of intensified bottom flow in the observed velocity fluctuations in the deep layer. This suggests that Kelvin waves are produced instead (Sheinbaum et al. 2010). In addition, 1-yr records from moorings in the BOC show the presence of TRWs only on the western slope, while on the eastern slope the fluctuations have higher frequencies and no bottom intensification (Kolodziejczyk et al. 2011). It is thought that the TRWs dissipate as they travel into the eastern side of the BOC due to the rough topography of the Campeche Knolls, and that edge waves are responsible for the fluctuations observed there (Kolodziejczyk et al. 2011). Also note that the slope in the eastern BOC opposes that of planetary  $\beta$ , hence the restoring force driving TRWs will be weaker there (Hamilton 1990).

No velocity observations exist in the deep layer adjacent to the northern Yucatan–Campeche slope to confirm the existence of TRWs propagating along that portion of the southern boundary. Hence, it is not clear if a boundary current is found all along the western GOM, and if it does exist, what is its driving mechanism in places where no clear evidence of TRWs exists?

On the other hand, the simple two-layer model of Hurlburt and Thompson (1980) and the analysis of hydrographic data by DeHaan and Sturges (2005) show indications of a boundary current driven by the inflow of cold, dense North Atlantic Deep Water (NADW) through the Yucatan Channel, which would tend to flow cyclonically against the slope as it mixes with the warmer water of the interior.

In the deep abyssal plain of the western basin, numerical studies suggest that the LC rings induce eddies in the bottom layer via vortex stretching, resulting in an anticyclone (cyclone) in the leading (trailing) edge moving westward and locked to the surface eddy (Hurlburt and Thompson 1982; Sturges et al. 1993; Welsh and Inoue 2000). Welsh and Inoue (2000) found that the deep cyclone survives longer than the anticyclone in the western Gulf, suggesting a mean cyclonic

abyssal flow. Tenreiro et al. (2018) show observational evidence of large-scale fluctuations of relative vorticity in the deep layer as expected from modons trapped below westward-moving LC rings. They also showed that positive vorticity accumulates in the abyssal plain as the LC rings dissipate against the western boundary, although the mooring array lacked enough resolution to fully resolve these deep eddies.

In this article, the large-scale patterns of the deep circulation of the Gulf of Mexico are described with data from a basinwide observational study. A large number of acoustically tracked subsurface floats (RAFOS; Rossby et al. 1986) were deployed throughout the GOM between July 2011 and September 2013, as part of the “Lagrangian study of the deep circulation of the deep Gulf of Mexico” study funded by the U.S. Bureau of Ocean Energy Management (BOEM). The dataset covers a 4-yr period, allowing investigation of the bottom-layer circulation over the entire GOM (Fig. 1a). A description of and preliminary results from the experiment can be found in Hamilton et al. (2016b). Links to reports and data are available at the BOEM Environmental Studies Program Information System (<https://marinecadastre.gov/espis/#/search/study/100029>, last accessed 25 November 2017).

The pseudo-Eulerian statistics of the bottom-layer flow of the GOM is obtained from the float dataset. Three patterns stand out in the binned statistics and are presented in the first part of section 3: a cyclonic boundary current, a mean cyclonic gyre in the abyssal plain in the western Gulf, and the very high eddy kinetic energy observed in the eastern Gulf. This study focuses on analyzing these features, with special emphasis on the western and southern basins, as these regions are historically under-sampled. The statistics are complemented with the data from the current meter moorings that were deployed during the same time period as the floats in the western GOM (Fig. 1b). In the second part of section 3, the data from the moorings and individual float trajectories are employed both to compare the Eulerian statistics, as well as to address the persistence and continuity of the boundary current and the deep cyclonic gyre. The names of the GOM physiographic provinces mentioned in the text are identified in Fig. 1b.

## 2. Data and methods

### a. Floats

A total of 152 RAFOS floats (121 ballasted for 1500 m and 31 floats for 2500 m) had useable missions spanning the period between July 2011 and June 2015. Record lengths for each float varied between 7 and 730 days. In

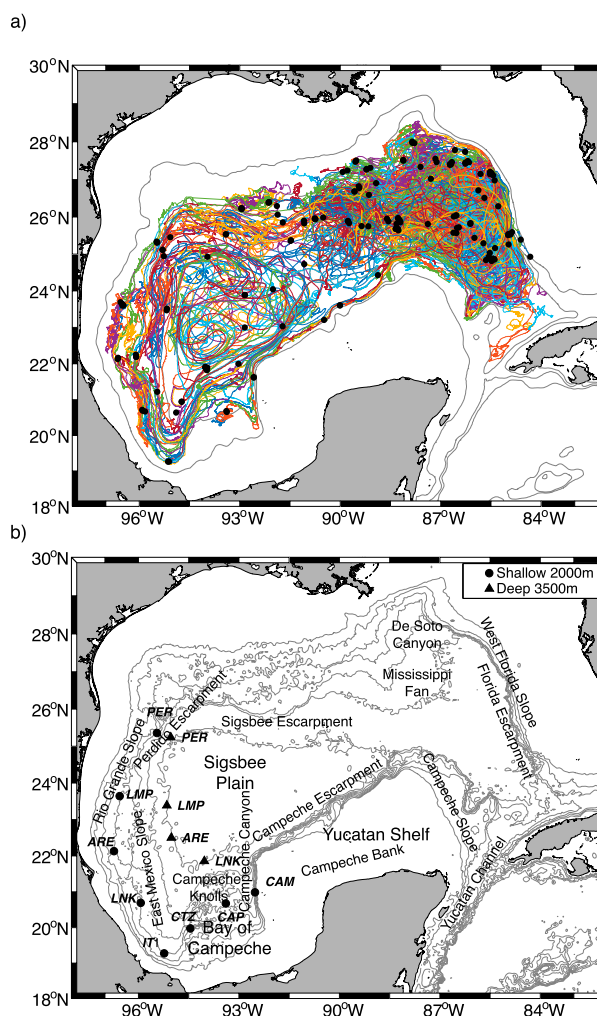


FIG. 1. (a) All RAFOS and APEX trajectories. Black dots represent first data collected. Smoothed isobaths at 1000, 2000, and 3000 m. (b) Positions of the Centro de Investigación Científica y de Educación Superior de Ensenada (CICESE)-Canek current meter moorings. Only moorings anchored at 2000-m (circles) and 3500-m (triangles) bottom depths are shown and used in this study. The three letters in italics represent the name of each cross-slope transect [Perdido (PER), Lamprea (LMP), Arenque (ARE), and Lankahuasa (LNK)] or individual moorings [Itinerante 1 (IT1), Coatzacoalcos (CTZ), Campeche Profundo (CAP), and Campeche (CAM)]. The principal physiographic provinces and geomorphic features of the Gulf of Mexico are presented (based on Martin and Bouma 1978). Isobaths are shown as black contours from [500:500:3500] m.

addition, six APEX profiling floats with RAFOS technology were also deployed in the same region and period, with a parking depth at 1500 m and vertical profiles scheduled every 14 days. All floats were acoustically tracked using an array of four sound source moorings, resulting in position records three times a day. The RAFOS floats also recorded temperature and pressure three times a day. All data were transmitted by Iridium

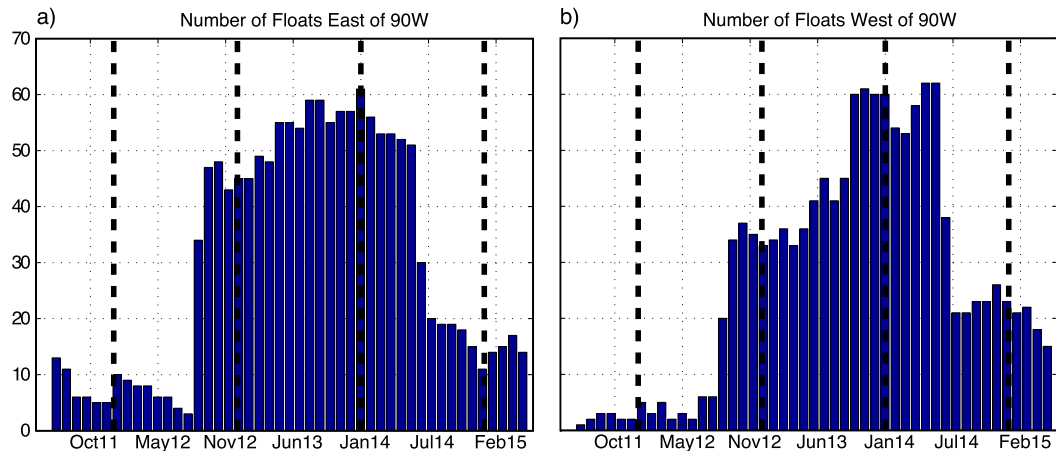


FIG. 2. Histogram of number of floats by month (a) east of  $90^{\circ}\text{W}$  and (b) west of  $90^{\circ}\text{W}$ .

satellite communications when the RAFOS float surfaced at the end of its mission, and every two weeks when the APEX float surfaced after sampling a vertical profile. For more details on the dataset, see Hamilton et al. (2016b). This dataset is available at the NOAA/AOML subsurface float observations archive ([http://www.aoml.noaa.gov/phod/float\\_traj/data.php](http://www.aoml.noaa.gov/phod/float_traj/data.php), last accessed 13 December 2017).

The trajectories of all floats are shown in Fig. 1a. Figure 2 shows the number of floats present in the western and eastern gulf at any given month during the period of the experiment. The 1500-m floats were deployed across the Gulf, while the 2500-m floats were deployed only in the eastern basin. For this reason, there is generally greater data density in the east than the west. The first year has little coverage, but from July 2012 on, both basins had between 20 and 50 floats recording data, with the eastern Gulf having the largest number of floats. Therefore, the statistics presented are representative of the period between September 2012 and June 2015, because much less data are available in the first year, particularly in the western Gulf. The 1500- and 2500-m floats were considered together, because not much difference is expected between those two layers given that, at least in the eastern basin, the currents are quite uniform with depth below 1000 m (e.g., Hamilton 1990).

### b. Moorings

An array of eight moorings along the 2000-m isobath and four at 3500 m were distributed along the western gulf (Fig. 1), measuring currents during the float experiment between 1 July 2011 and the end of May 2015. These moorings were equipped with a suite of acoustic profilers and point current meters to measure currents over the whole water column. In particular to measure

currents between 1000 and 1800 m, both the 2000- and 3500-m moorings were equipped with downward-looking 75-kHz acoustic profilers at 700 m that measured currents between 700 and 1200 m with a 16-m depth resolution every half hour. Below 1200 m, on both types of moorings, fixed-point current meters (Nortek AQUADOPS or Aanderaa RCM-11 or SeaGuards) were installed at 1300-, 1500-, and 1800-m depths, measuring currents at 15- or 30-min time intervals, depending on the instrument used. Currents measured with all instruments were processed to obtain hourly sampled series. Based on these series, the mean velocity and variability ellipses measured at 1500 m depth were calculated for all moorings. To determine the significance of the mean current estimates, decorrelation time scales were estimated from the autocorrelation function of the principal axis time series. The decorrelation scales for the 1500-m currents at the 2000-m moorings are similar to the ones obtained for the binned float data, varying from 5 to 11 days except for mooring CAP, on the southern flank, that has a decorrelation scale of around half a day (Fig. 1b). For the 3500-m moorings, the currents at 1500 m have longer decorrelation scales varying from around 27 days at LMP-3500 to 60 days at ARE-3500. Table 1 summarizes the mooring data series measured at 1500 m, including the degrees of freedom (DOF), calculated as the length of the time series divided by the corresponding decorrelation time scale. This dataset is proprietary and made available upon request to review the results of this work.

### c. Gridded fields from the float data

The study area was divided into a regular grid of  $0.5^{\circ} \times 0.5^{\circ}$  overlapping boxes, centered on a  $0.25^{\circ} \times 0.25^{\circ}$  grid. The overlap provides spatial smoothing of the final fields. To establish statistical confidence, the

TABLE 1. Description of mooring velocity time series at 1500 m.

Mooring name	Series length (days)	Decorrelation time scale (days)	DOF
PER-2000	1425	8	171
LMP-2000	1088	5	209
ARE-2000	649	8	80
LNK-2000	782	9	90
IT1-2000	1161	10	112
CTZ-2000	1106	7	162
CAP-2000	1042	0.4	2502
CAM-2000	782	11	69
PER-3500	839	37	23
LMP-3500	814	27	31
ARE-3500	430	61	7
LNK-3500	412	29	14

degrees of freedom for each bin were estimated based on the integral time scale ( $T$ ; Lacasce 2008). This scale was estimated for each float trajectory and ranged between 0 and 15 days. The average time scale for all floats lies between 1 and 6 days depending on the region of the Gulf (Hamilton et al. 2016b). Hence, 5 days were used as the time scale at which data points were considered independent, and the DOF were based on the number  $N$  of unique days that have observations in each bin, such that  $\text{DOF} = N/T$ . If a bin has three floats that were recording data during the same 5-day period, that counts as five unique days, and hence  $\text{DOF} = 1$ . If, by contrast, each of the three floats visited the area in different months and recorded data for five continuous days,  $N = 15$  and the corresponding  $\text{DOF} = 3$ . Figure 3 shows the number of data points and number of DOF for each bin. Only bins with more than five degrees of freedom are considered in the results. The eastern Gulf was the most sampled region, with more than 75 DOF in most bins, followed by the boundary of the western Gulf

( $\sim 70$  DOF). The abyssal plain and the deep Bay of Campeche were the least sampled regions ( $< 45$  DOF).

Mean velocities and standard deviation ellipses were estimated for each bin in the case of the float data, and at each mooring for the current meter data, and a Student's  $t$  test was used to check if the mean velocities were significantly different than zero ( $p = 0.05$ , Emery and Thomson 2001). The mean kinetic energy (MKE) was calculated as  $\text{MKE} = \frac{1}{2}(U^2 + V^2)$ , where  $U$  and  $V$  are the mean zonal and meridional velocities, while the eddy kinetic energy (EKE) was estimated as half the sum of the variances along the major and minor axes.

Potential vorticity is expected to play a significant role in the dynamics of the lower layer. Therefore, planetary potential vorticity contours  $f/H$  are plotted on all maps, where  $f$  is the local Coriolis frequency and  $H$  is the bottom depth ( $f/H$  contours are also known as barotropic geostrophic contours; Dewar 1998). Formally, one should use the thickness of the bottom layer and not the full water column depth to determine potential vorticity of the abyssal flow. Nevertheless, the mean map of potential vorticity for the bottom layer as estimated from the profiling floats shows the same mean pattern as the barotropic geostrophic contours estimated with the total depth, with closed contours of low potential vorticity west of  $88^\circ\text{W}$  and strong gradients over the continental slope (Fig. 4-13 in Hamilton et al. 2016b; see also Hamilton et al. 2017, manuscript submitted to *J. Phys. Oceanogr.*).

### 3. Results and discussion

#### a. Gridded fields

The gridded maps with the statistics of the velocity field at 1500 m obtained with the float and mooring data are shown in Figs. 4–6. The main features that stand out

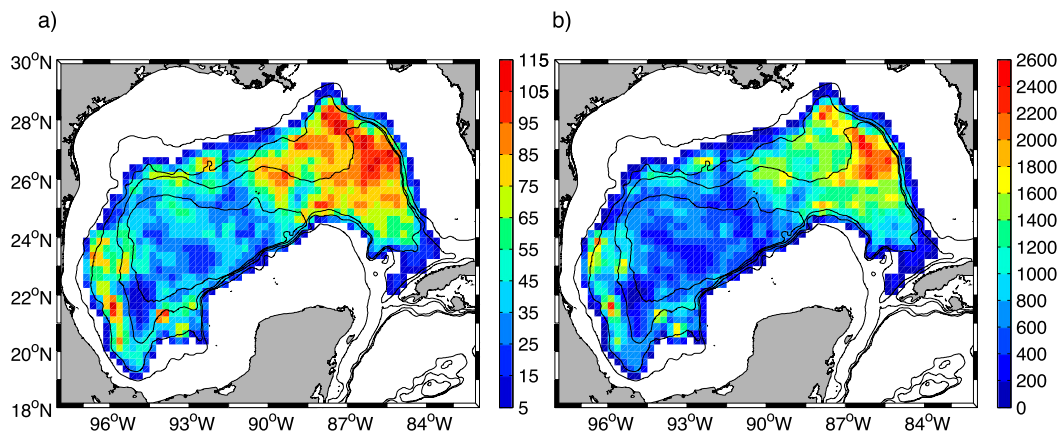


FIG. 3. (a) Number of observations and (b) degrees of freedom for each bin. Geographical bins are  $0.5^\circ \times 0.5^\circ$  in size, centered on a  $0.25^\circ$  grid. Only bins with at least five degrees of freedom are plotted. Isobaths are shown as black contours at 1000, 2000, 3000, and 3500 m. Note that the scales for the two plots are different.

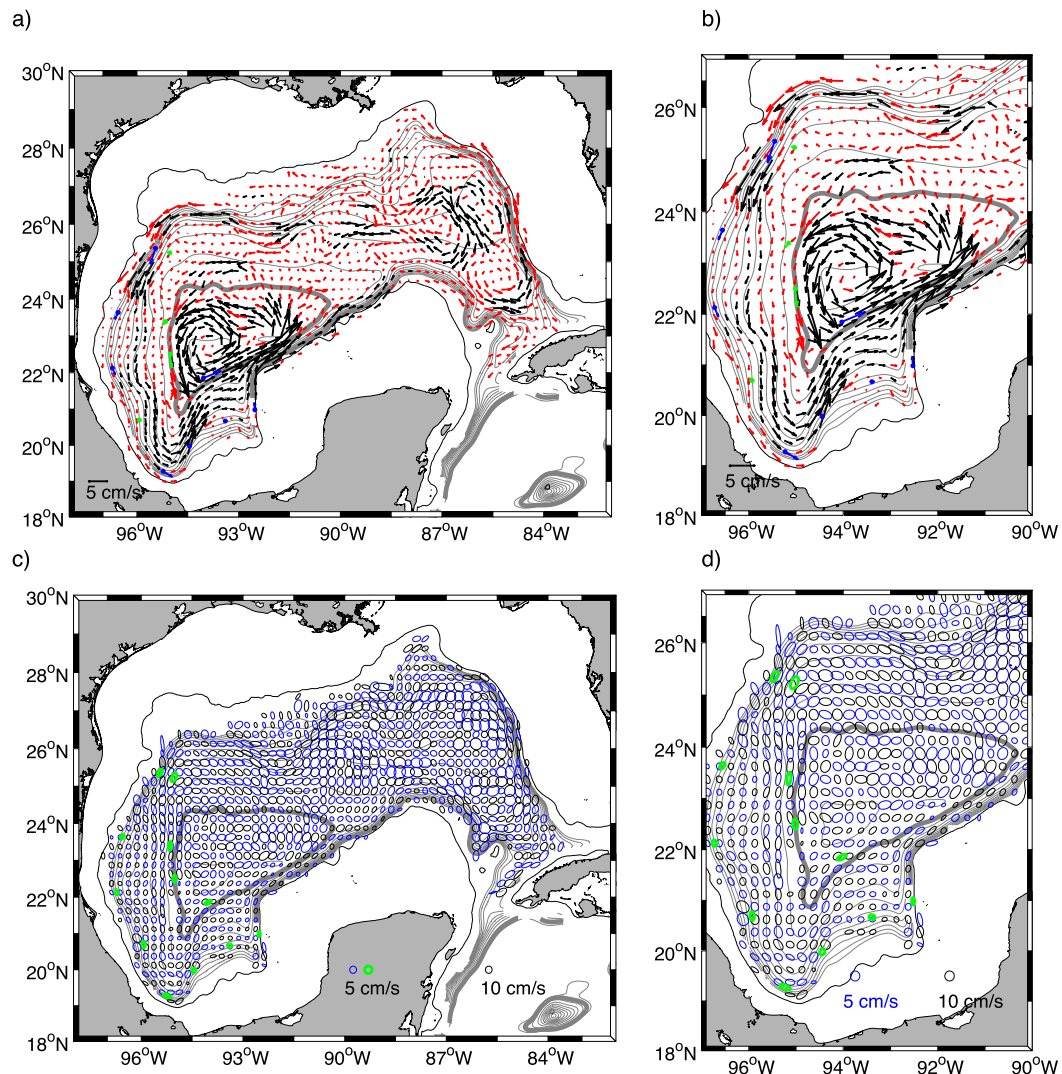


FIG. 4. (a),(b) Mean velocity vectors. Black (red) arrows indicate float bin averages significantly (not) different from zero at the 95% confidence level and blue (green) arrows indicate the same but for the mooring averages. (c), (d) Standard deviation ellipses for floats (blue) and moorings (green). Black ellipses (from floats) have a different scale. Planetary potential vorticity ( $f/H$ ) contours in gray ( $[1.52:0.2:3.5] \times 10^{-8} \text{ m}^{-1} \text{ s}^{-1}$ ), where  $f$  is the local Coriolis parameter and  $H$  is the bottom depth. Closed  $f/H$  contour  $1.61 \times 10^{-8} \text{ m}^{-1} \text{ s}^{-1}$  shown with a thick gray line. Black contour shows the 1000m isobath. Gridded fields produced and plotted using jLab routines (Lilly 2017).

are a mean cyclonic boundary current of about  $3 \text{ cm s}^{-1}$  around most of the Gulf, more evident in the western GOM (Fig. 4a), a mean cyclonic gyre in the abyssal plain of the western basin spinning at about  $5 \text{ cm s}^{-1}$  (Fig. 4b), and high EKE observed in the eastern GOM ( $>80 \text{ cm}^2 \text{ s}^{-2}$ ; Fig. 5a). Also noticeable is the rapid decay of the EKE toward the western basin, with lower values observed in the BOC and the central western boundary ( $<30 \text{ cm}^2 \text{ s}^{-2}$ ; Fig. 5a) and a localized hotspot of relatively high EKE off the Campeche Escarpment around  $91^\circ \text{W}$  ( $40\text{--}70 \text{ cm}^2 \text{ s}^{-2}$ ; Fig. 5b). The gridded dataset is available at the BOEM data archive ([https://opendata.](https://opendata.boem.gov/GriddedFields_1500m_floats_CF.nc)

[boem.gov/GriddedFields\\_1500m\\_floats\\_CF.nc](https://opendata.boem.gov/GriddedFields_1500m_floats_CF.nc), last accessed 13 December 2017).

Note that standard deviation ellipses in the gridded fields are rather circular and are only slightly aligned with topography in some cases (Figs. 4c,d). The places where ellipses are most aligned along the slope coincide with regions of steep slopes along the boundary: the Florida Escarpment, the northwestern gulf, along the 2000- and 3000-m isobaths north to south along the East Mexico Slope, the Campeche Escarpment, and the northwestern Cuban shelf. The MKE differs from the EKE (Figs. 5, 6), in that the MKE shows the strongest

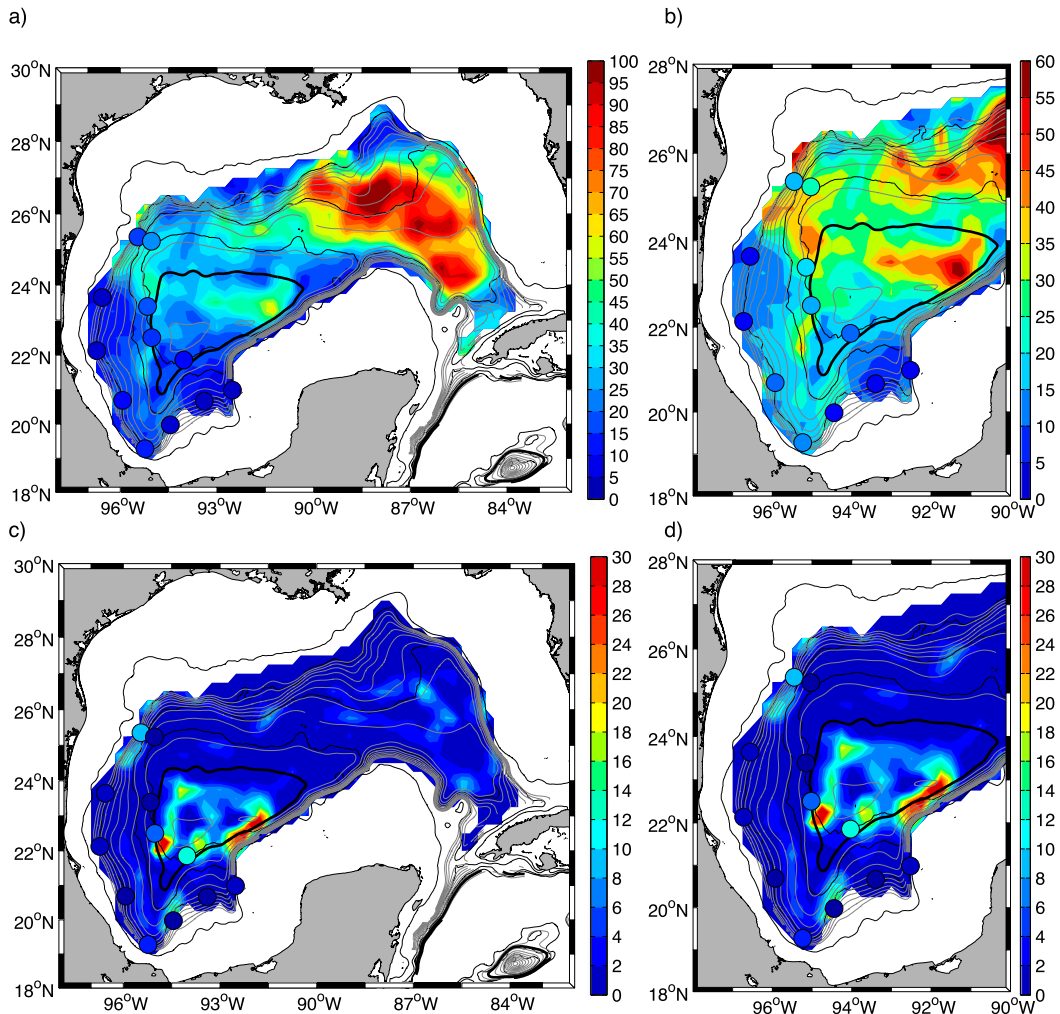


FIG. 5. (a),(b) EKE ( $\text{cm}^2 \text{s}^{-2}$ ) for floats (color map) and moorings (colored dots). Note the color scales are different. (c),(d) MKE ( $\text{cm}^2 \text{s}^{-2}$ ) for floats (color map) and moorings (colored dots). Planetary vorticity ( $f/H$ ) contours as in Fig. 4, with closed contour  $1.61 \times 10^{-8} \text{m}^{-1} \text{s}^{-1}$  shown with thick black line. Isobaths are black contours at 1000, 2000, 3000, and 3500 m.

persistent flow in an annulus shape that corresponds to the deep gyre in the abyssal plain, at about  $23^\circ\text{N}$ ,  $93^\circ\text{W}$ , hereafter called the Sigsbee Abyssal Gyre (SAG). This choice was made based on the name of the abyssal plain over which it flows, which in turn was named after Charles Dwight Sigsbee, who made high-resolution and accurate soundings that lead to the first modern bathymetric map of the Gulf of Mexico and the Caribbean (NOAA 2017).

### 1) GRIDDED FLOAT DATA VERSUS MOORING STATISTICS

In the western Gulf, the standard deviation ellipses for the moorings coincide fairly well with the ones obtained from the binned float data at that nearest  $0.5^\circ$  square, although the float-derived statistics slightly overestimate

the variability observed by the moorings (Table 2). In general, the mooring data show more anisotropic variability than the floats near the boundaries, although both datasets show small and rather circular ellipses in the central western boundary and in the region of the Campeche Knolls.

The mean velocities obtained for the moorings and the gridded fields also show similar magnitudes and direction, with the largest means observed in the north-western boundary and the southern edge of the cyclonic gyre. In the central western boundary, the moorings show significantly higher means. The most noticeable difference between both datasets is found in the central BOC (mooring CTZ), where the gridded fields show a strong mean boundary current that represents over 30% of the total kinetic energy of the flow and the mooring

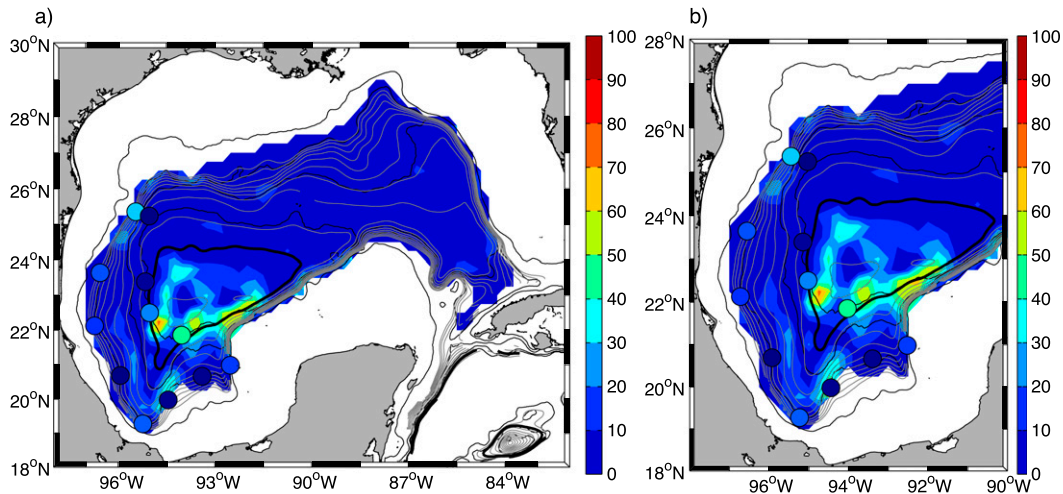


FIG. 6. Percentage of mean to total kinetic energy [ $\text{MKE}/(\text{MKE} + \text{EKE}) \times 100$ ] for floats (color map) and moorings (colored dots). Isobaths and  $f/H$  contours as in Fig. 4.

shows an order of magnitude smaller EKE and nearly null mean flow. This is likely due to the fact that the CTZ mooring may be missing most of the boundary current flow due to its location, as will be shown with the analysis of the float trajectories of section 4c(2).

## 2) EASTERN BASIN

In the eastern basin, the mean flow shows three recirculation cells, two cyclonic to the southeast and northeast and one anticyclonic to the northwest (Fig. 4a), with mean speed for all three of approximately  $3 \text{ cm s}^{-1}$ . The convergence due to the dipole in the northern basin results in relatively high and significant mean flow toward the south. The northern dipole appears to be a persistent feature, since it has been observed previously with moorings (Hamilton et al. 2015, 2016a). These authors associate its existence to potential vorticity conservation

due to stretching/compression of the deep layer as the Loop Current expands toward the northern slope. The very high EKE observed in the eastern basin has been reported previously (Fig. 6; Hamilton 2009), and it has been mostly attributed to baroclinic instabilities in the Yucatan current and Loop Current expansion generating deep eddies (Donohue et al. 2016; Sheinbaum et al. 2016), although vorticity fluxes from the Caribbean, as well as those generated by the interaction of the Yucatan current with coastally trapped waves arriving from the southern GOM boundary, can also play a role in the production of the barotropic cyclonic eddies that appear off the eastern corner of the Campeche Bank (Jouanno et al. 2016; Sheinbaum et al. 2016). Numerical model results suggest that once these deep cyclones are formed, they transfer energy westward; either as they translate toward the deep basin or by generating TRWs as they

TABLE 2. Comparison of current meter mooring statistics and binned float statistics, using the bin whose center is closest to the mooring. Velocity direction in degrees due east.

Mooring name	Mean velocity				Variance ellipses				Eccentricity	
	Magnitude ( $\text{cm s}^{-1}$ )		Direction ( $^{\circ}$ )		Mayor Axis ( $\text{cm s}^{-1}$ )		Minor Axis ( $\text{cm s}^{-1}$ )		Mooring	Float
	Mooring	Float	Mooring	Float	Mooring	Float	Mooring	Float		
PER-2000	4.5	2.7	-108	-126	5.7	7.1	2.5	4.1	0.9	0.8
LMP-2000	2.4	0.3	-115	-108	3.4	3.7	2.2	2.9	0.8	0.6
ARE-2000	2.3	0.9	-61	-80	3.1	3.7	2.3	3.3	0.7	0.5
LNK-2000	0.1	1.3	154	-90	4.4	4.9	2.2	4.3	0.9	0.5
IT1-2000	3.1	1.1	-27	-9	5.5	5.1	2.1	2.9	0.9	0.8
CTZ-2000	0.9	5.8	129	70	3.1	5.1	2.6	3.8	0.6	0.7
CAP-2000	0.5	0.4	10	22	2.9	3.2	2.5	2.6	0.5	0.6
CAM-2000	1.9	1.7	93	96	3.5	3.5	1.5	3.0	0.9	0.5
PER-3500	0.8	1.5	-172	-125	6.4	6.4	3.2	4.6	0.9	0.7
LMP-3500	1.0	0.7	-125	-137	6.1	7.0	1.9	3.2	1.0	0.9
ARE-3500	3.0	3.3	-82	-80	5.0	7.3	2.4	3.4	0.9	0.9
LNK-3500	4.6	3.0	24	29	4.9	4.9	2.0	3.0	0.9	0.8

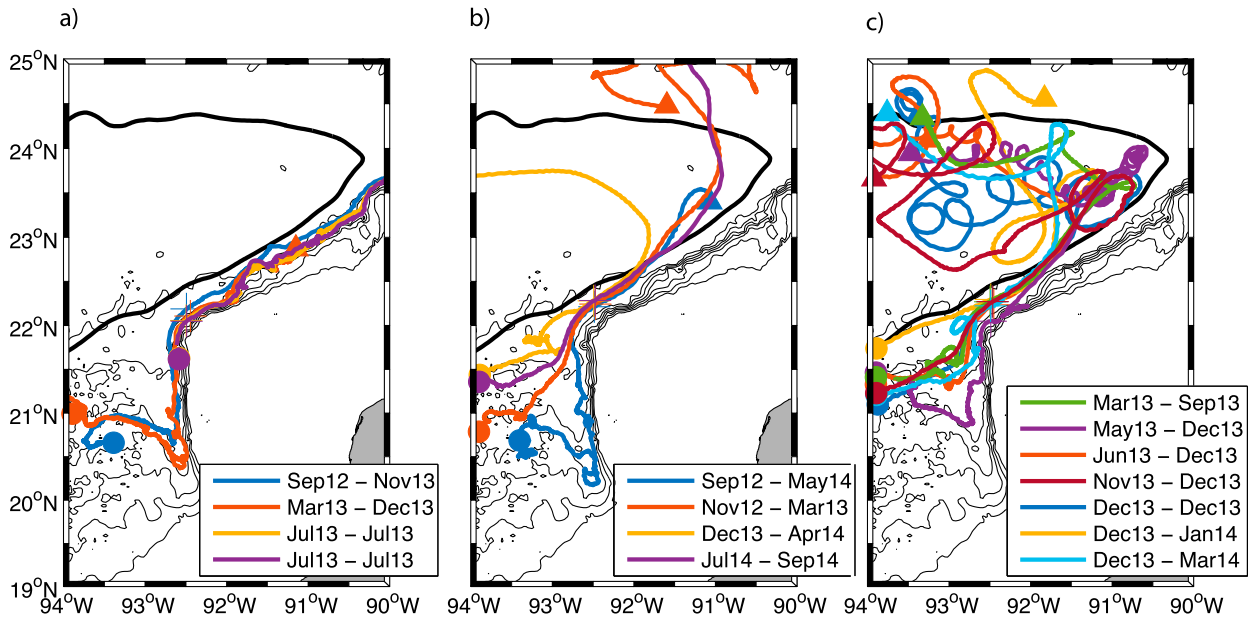


FIG. 7. Boundary current separation. Isobaths are shown as gray contours from [500:500:3500] m. The  $f/H$  contour of  $1.61 \times 10^{-8} \text{ m}^{-1} \text{ s}^{-1}$  is marked with a thick black line. Dots (triangles) mark first (last) data points. Dates indicate time interval between first data point and time when float reached point of separation right after turning around the northwest corner of Campeche Bank ( $\sim 92^\circ\text{W}$ ; marked with a cross). (a) Trajectories following the Campeche Escarpment toward the east. (b) Trajectories showing boundary current separation without looping behavior (c) Trajectories showing boundary current separation with looping behavior, indicating the presence of eddies.

interact with the northern slope (Oey 2008). A more detailed study of the coupling of the upper- and lower-layer flows in this basin as observed by the float dataset is underway. Hence, we will now focus our attention to the western GOM.

### 3) BOUNDARY CURRENT

Evidence of a mean deep cyclonic boundary current is observed everywhere except in the northeastern Gulf (Mississippi Fan and De Soto Canyon, east of  $91^\circ\text{W}$ ; Fig. 4a). Regions where the boundary current appears more clearly coincide with high gradients of potential vorticity  $f/H$ , such as in the northwest boundary (Perdido Escarpment), in the Bay of Campeche, and along the Campeche and Florida Escarpments. The highest mean velocities ( $>5 \text{ cm s}^{-1}$ ) and mean kinetic to total kinetic energy ratios, which is a measure of the importance of mean flow ( $>30\%$ , Fig. 6), of the boundary current are observed in the northwestern Gulf (between  $24^\circ$  and  $25^\circ\text{N}$ ), in the central BOC (where the flow turns north at  $\sim 94.5^\circ\text{W}$ ), and most notably on the west corner of the Campeche Escarpment, where maximum speeds of up to  $8 \text{ cm s}^{-1}$  and energy ratios of 65% can be found (Figs. 4–6).

### 4) CAMPECHE GYRE

Floats show no clear expression of the semipermanent cyclonic gyre in the bottom layer of the Bay of Campeche, as

was suggested by Pérez-Brunius et al. (2013). Instead of a closed cyclonic gyre within the western BOC, floats tend to flow along the boundary and then turn east along the Campeche Escarpment. Some floats go around the narrow Campeche Canyon in the eastern Bay of Campeche, before making a sharp eastward turn on the west corner of the Campeche Escarpment (Fig. 7). Hence, if the surface-intensified Campeche gyre is an equivalent barotropic flow, at 1500 m it is weak compared to the deep boundary current.

#### b. Separation of the boundary current in Campeche Escarpment

The mean boundary flow speeds up as it exits the Bay of Campeche and continues east along the steep slope of the Campeche Escarpment, maybe as a result of the convergence with the flow of the deep basin's cyclonic gyre (Fig. 4b). Part of the boundary flow separates at  $\sim 92^\circ\text{W}$ , turning northward, then westward as it enters the abyssal plain, feeding into the cyclonic gyre (Figs. 4b, 7). The high MKE observed along the western portion of the Campeche Escarpment coincides with the region before the point of separation, while the high EKE energy spot is observed downstream of where the flow detaches from the continental slope (Figs. 5, 6).

Figure 7 shows the process of separation observed by the trajectories of the 15 floats that flowed along the boundary in the BOC. These floats passed through the

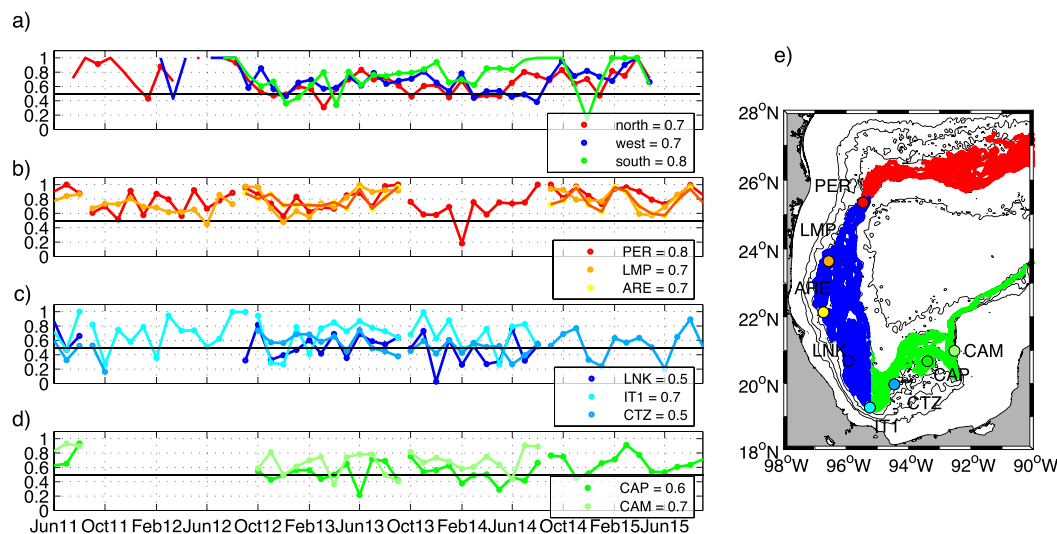


FIG. 8. Cyclonic velocity observations along the boundary. (a) Time series of the fraction of smoothed float velocity observations along the boundary in the cyclonic sense in three regions of the western Gulf: northern slope (red), western slope (blue), and Campeche Bank slope (green). Circles indicate the points where there are more than 100 observations. Monthly fraction of cyclonic flow at 1500 m from moorings in (b) northern, (c) western, and (d) southeastern continental slope. Legends in (a)–(d) show the corresponding time-mean value. (e) Locations of float velocity observations (small dots in red, blue, and green) used in (a) and mooring positions (colored circles) corresponding to (b)–(d). Isobaths as in Fig. 7.

region between March 2013 and September 2014 (five floats did so between December 2013 and January 2014). All 15 floats converged at the west corner of the Campeche Escarpment and continued in a strong boundary jet, suggesting it is a persistent phenomenon, not an isolated event. The speeds in some (not all) floats embedded in this current increase from 5 to  $35 \text{ cm s}^{-1}$  as the corner is navigated. Four floats continue east along the boundary, but the other 11 exit the boundary at  $\sim 92^\circ\text{W}$ , coinciding with the location of a topographic bump. As they enter the abyssal plain, 7 of the 11 floats end up to varying degrees in westward-moving anticyclones. Preliminary analysis finds no evident relation between this subsurface feature and the altimetric sea surface height field, so it is not clear if the separation in this region is connected to the upper-layer dynamics (Hamilton et al. 2016b). The separation process and its apparent relation to the deep eddies is a remarkable discovery of the float program and is the subject of ongoing research.

### c. Persistence and continuity of the boundary current in the western basin

#### 1) PERSISTENCE OF CYCLONIC FLOW ALONG CONTINENTAL SLOPE

Although the boundary current appears in the mean velocity field, it is not necessarily a persistent continuous structure. Figure 8 shows time series of the monthly

fraction of float and mooring observations that indicated cyclonic boundary current circulation on the continental slope. In the case of the floats, this analysis was performed in three regions: the northern slope, western slope, and Campeche bank slope (Fig. 8a). Figure 8e shows the locations of the float velocity data used, which include only float velocities inshore of the 3000-m isobath. The float velocity observations were first rotated into along- and across-isobath components, where the bathymetric gradient was estimated at each float position by fitting a plane to the bathymetric data in a  $\sim 50 \text{ km} \times 50 \text{ km}$  box centered at the float position. The along-isobath velocity component was then smoothed with a third-order low-pass Butterworth filter with a 30-day cutoff period, run forward and backward to eliminate phase shifts. Finally, for each 30-day time period, the numbers of observations with counterclockwise (cyclonic) sense of flow were counted.

In the case of the moorings along the 2000-m isobath, the hourly velocity data were rotated along their principal components, which are mainly aligned with topography (Fig. 4d). The fraction of observations showing cyclonic flow on each 30-day window is graphed in Figs. 8b–d. In both the float and mooring fractions, the 0.5 level is highlighted with a horizontal black line: this is where there are an equal number of observations with clockwise and counterclockwise observations.

In general, the time series of the floats and moorings are consistent with the Eulerian mean statistics, in that ~70% of the time there were more observations in the cyclonic direction in the northern and western slopes. In the Bay of Campeche, the moorings and floats differ in that all except the southern (IT1) and eastern (CAM) moorings show mostly back-and-forth motion, while all floats show a high tendency for cyclonic flow (Fig. 8). Since most floats that are present in the Bay of Campeche were deployed in the northern and central continental slope (Fig. 1a), the tendency of cyclonic flow could be due to sampling bias given that only floats embedded in such flows would be able to enter the Bay of Campeche. The fact that there was a steady stream of floats in the region from June 2012 until the end of the record suggests the result is not biased. As will be shown later, the LNK, CTZ, and CAP moorings are located shoreward of the trajectories of floats more effectively advected by the boundary current (CTZ, CAP; see Fig. 11) or in regions where floats tended to stall and have more erratic behavior (LNK, CAP; see Fig. 11).

Although both datasets show multimonth periods when there was a high fraction of cyclonic boundary current-like behavior, extended time periods characterized by more back-and-forth motion were observed. For example, between October 2012 and March 2013, a tendency closer to back-and-forth motion (with periods longer than 30 days) was reported by the floats in all the regions (Fig. 8a), coinciding with a drop in the fraction of cyclonic flow in nearly all of the moorings (Figs. 8b–d).

It is noted that six Loop Current eddies entered the western region in the time period analyzed here (see Figs. 3–28 and 5–28 in Hamilton et al. 2016b). The last one was Kraken, which dissipated around May 2014. Past that period, no other Loop Current eddies made it into the western basin during the time of the experiment. This relatively quiet period coincides with a high fraction of cyclonic flow in the northern and central boundary and suggests that the LC eddies play a role in the disruption of an otherwise cyclonic boundary current around the western gulf, probably inducing topographic Rossby waves. More analysis is underway to confirm this relationship.

## 2) CONTINUITY OF THE BOUNDARY CURRENT AND TRANSIT TIMES

The results above suggest that the boundary flow is episodic in character. Nevertheless, there are periods when this boundary current is continuous, as shown by floats traveling far along this flow in nearly all regions of the GOM, including the northeastern slope and Florida Escarpment (Fig. 9). For example, float 1081 (drifting at 2500 m) was trapped in a coherent boundary flow all around the western Gulf along the 3000-m isobath

(Fig. 9a). It joined the boundary current in March 2012 at the central northern slope and continued all the way to the BOC. Unfortunately, it got stuck to the bottom in October 2012 and remained in the same spot for 5 months until its mission ended in March 2013. The only region that never showed a deep continuous flow was under the Loop Current where it enters and exits the Gulf (i.e., along the Yucatan Channel and Straits of Florida).

Figures 10 and 11 show the trajectories of floats that were found in different regions over the continental slope in the western Gulf of Mexico, with trajectories longer than 30 days in each of the four regions analyzed (northern, western, and BOC slopes and Campeche Escarpment). These are floats that either were deployed in the region in question or entered it at some point of their lifetime. Figures 10 and 11 show that floats travel along the boundary current for a given period of time and do one of the following: slow down and stall, reverse, show back-and-forth motion or looping behavior, or get trapped in small eddies.

Thirteen floats entered the western Gulf via the northern boundary or were originally deployed there, and all but one showed a net cyclonic displacement that took them south of 23°N in the western GOM (Fig. 10, top panels). Nevertheless, large excursions from a cyclonic boundary flow are seen in most floats, and only seven of them remained over the continental slope at all times (bottom depths <3500 m). The other four followed intricate paths over the abyssal plain before returning to the western boundary on their way to the southern GOM. The average travel time to get south of 23°N for the seven floats that stayed within the continental slope is 355 days.

Likewise, of the 20 floats that were either deployed or entered the western slope south of 24°N with trajectories longer than 30 days, all had a net southward displacement over the slope and entered into the Bay of Campeche, except for two that traveled northward (Fig. 10, bottom panels). Again, high variability is observed on the paths taken by the floats, but they are all embedded in a southward boundary flow, and it takes an average of 305 days to travel from 24° to 21°N.

There were 27 floats in the BOC along the boundary (Figs. 11a–d): all but three had a net cyclonic displacement over the continental slope and either stopped transmitting within the Bay of Campeche or turned eastward around the western tip of the Campeche Escarpment. The floats in this region showed less erratic paths than in the western and northwestern slopes, but looping and back-and-forth motions were embedded within the boundary flow. This behavior was more frequent for floats traveling close to the 2000-m isobath over the western BOC slope, and over the rugged region of the East Mexico Slope and Campeche Knolls. Also,

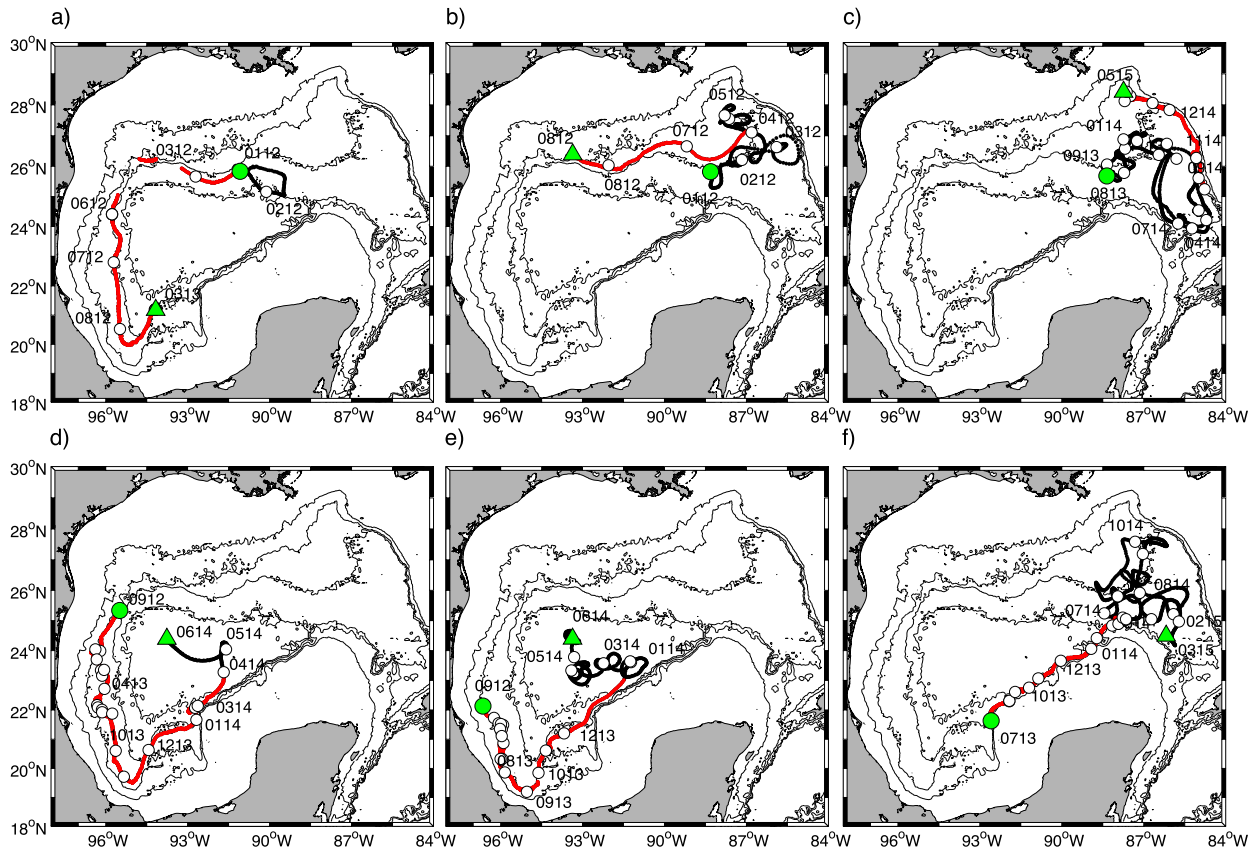


FIG. 9. Trajectories of floats showing flow along a boundary current. Green circles (triangles) represent location of first (last) data collected. The part of the trajectory along the boundary current is in red. Monthly date tags (mmdd) correspond to the white circles. Isobaths are shown as black contours at 1000, 2000, 3000, and 3500 m. Float in (a) was drifting at 2500 m; the floats for the rest of the panels were 1500 m.

floats traveling close to the 2000-m isobath entered Campeche Canyon, while those closer to the 3000-m isobath continued a faster and more direct route toward the Campeche Escarpment. The average transit time for the six floats that made it around the BOC and onto the northwestern slope of the Yucatan shelf is  $\sim 230$  days.

It is likely that the much larger mean flow in the gridded-float data compared to that measured by the CTZ current meter is due to the mooring being located shoreward of the main boundary current flow at 1500 m, since all float trajectories passed offshore of the mooring position (Figs. 11a–d).

The least sampled region is the Campeche Escarpment downstream of the point of separation of the boundary current (Figs. 11e–g). Only nine floats with trajectories longer than 30 days were found over the Escarpment east of  $92^{\circ}\text{W}$ . All but two remained within the boundary until they stopped transmitting or passed the northeastern tip of the Yucatan shelf. Of the four floats that traveled eastward past the tip of the Campeche Bank, two continued along the boundary heading

toward the Yucatan Channel, with one stopping its record on its way there, while the other detached from the boundary at  $\sim 86^{\circ}\text{W}$  (Fig. 11, bottom panel). It took 298 days for the two floats that traveled from the northern boundary (west of  $92^{\circ}\text{W}$ ) to the point of separation to the northeastern tip of the Yucatan Shelf. Table 3 shows the average transit times through each region.

The above analysis shows that, although there is significant variability embedded within the mean boundary current, this flow allows a pathway for water to move around the western GOM, taking an average of  $\sim 2$  years for floats to travel from the northern boundary (west of  $92^{\circ}\text{W}$ ) to the point of separation near  $92^{\circ}\text{W}$  over the Campeche Escarpment. Although very few trajectories were found over the northern slope of the Campeche Bank, there is evidence that this boundary flow continues onto the eastern slope of the Yucatan Peninsula.

#### d. Sigsbee Abyssal Gyre

A mean flow in a cyclonic gyre is observed in the deep abyssal plain of the western Gulf (Sigsbee Plain,  $>3500$  m),

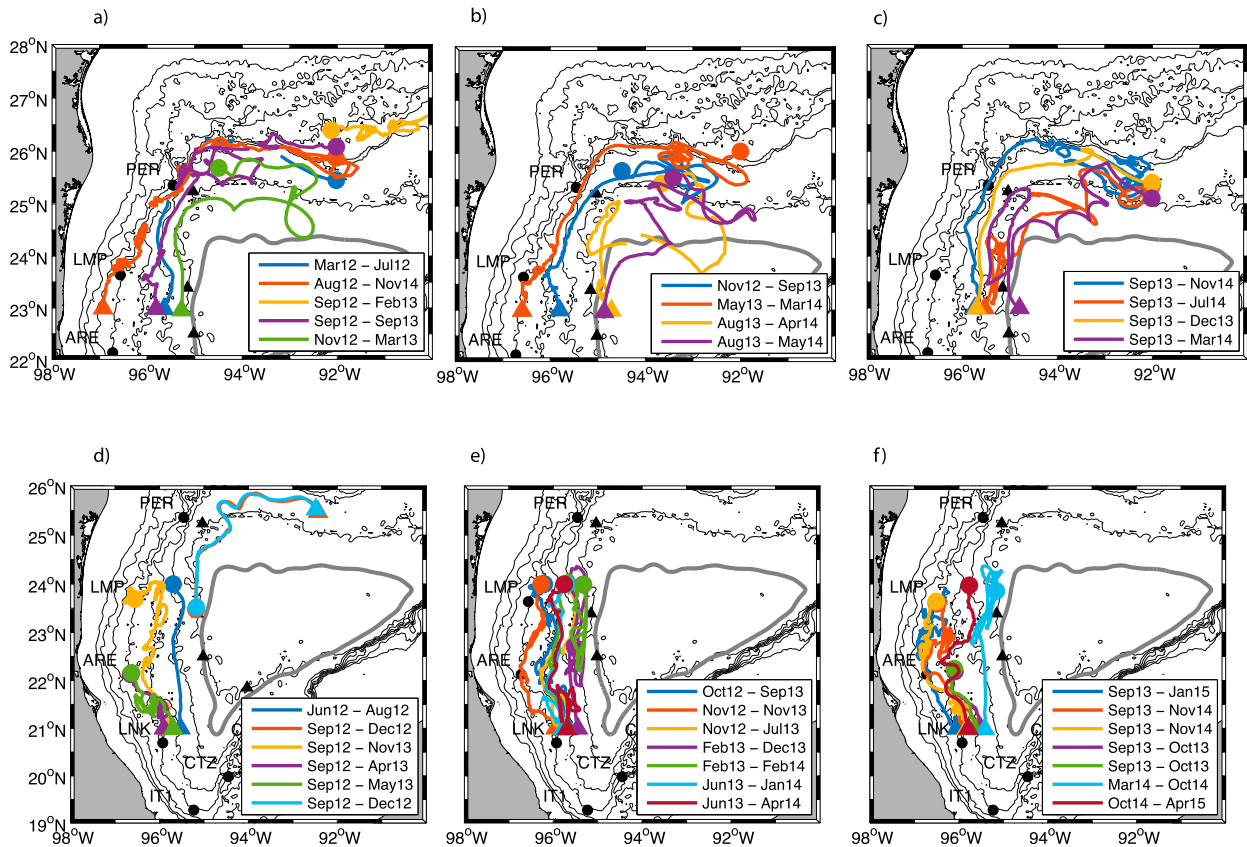


FIG. 10. Piecewise trajectories in boundary current over (a)–(c) northern and (d)–(f) western continental slope. Dots (triangles) show position of first (last) data point within the region. Dates show period between first and last data point for each float. Black circles (triangles) indicate position of 2000 m (3500 m) current meter moorings. Isobaths are shown as black contours from [500:500:3500] m. The  $f/H$  contour of  $1.61 \times 10^{-8} \text{ m}^{-1} \text{ s}^{-1}$  is marked with a thick gray line.

although it is much more clearly defined in a cell centered at  $22.5^\circ\text{N}$  and  $94^\circ\text{W}$  and located between  $22^\circ$  and  $24^\circ\text{N}$  (Fig. 4b), which we have named the Sigsbee Abyssal Gyre. The gyre has average speeds of  $5 \text{ cm s}^{-1}$ . This feature is the one that has the highest MKE and  $\text{MKE}/(\text{MKE} + \text{EKE})$  ratio in the entire basin ( $20\text{--}35 \text{ cm}^2 \text{ s}^{-2}$  and  $40\%\text{--}70\%$ , respectively; Figs. 5a,b and 6b); hence, it appears as the most persistent pattern of the mean circulation of the deep Gulf, although it is also the least sampled region by the floats ( $\text{DOF} < 55$ ) and moorings. Nevertheless, of the 66 floats deployed in the western GOM ( $< 90^\circ\text{W}$ ) with records longer than 2 months, 13 were deployed within the cyclonic gyre and 22 (42%) enter it at a later time, passing through the region where the gyre merges with the Campeche Escarpment. That is, nearly half the floats deployed outside of the abyssal plain end up in the gyre. The deep moorings also support the idea of a mean cyclonic flow.

To analyze the persistence of the cyclonic flow in the gyre, an analysis analogous to the one done for the boundary current was carried out. The float trajectories were selected within the closed  $f/H$  contour that

contains the SAG and divided in three regions (north, west, and south; Fig. 12e). The fraction of float data with low-pass-filtered velocities flowing in a cyclonic sense were estimated (cutoff frequency of 30 days; Fig. 12a). Note that although most months have less than 100 observations, all three regions showed cyclonic flow over 60% of the time. This is corroborated by the current meter data in the western and southern regions of the gyre (Figs. 12b–d), with the ARE and LNK moorings showing cyclonic flow over 70% and 80% of the time, respectively.

Both the mean flow and individual float trajectories suggest that most of the flow that separates from the boundary in the northwestern Campeche Escarpment feeds into the SAG. This is clear from the floats that are trapped in westward moving anticyclones upon entering the abyssal plain (Fig. 7c). Do note that only one of the floats that left the boundary makes a clear path following the mean field of the cyclonic gyre, and that the rest of the floats that do not exhibit eddying behavior end up traveling northward (Fig. 7b). Hence, it may well be that

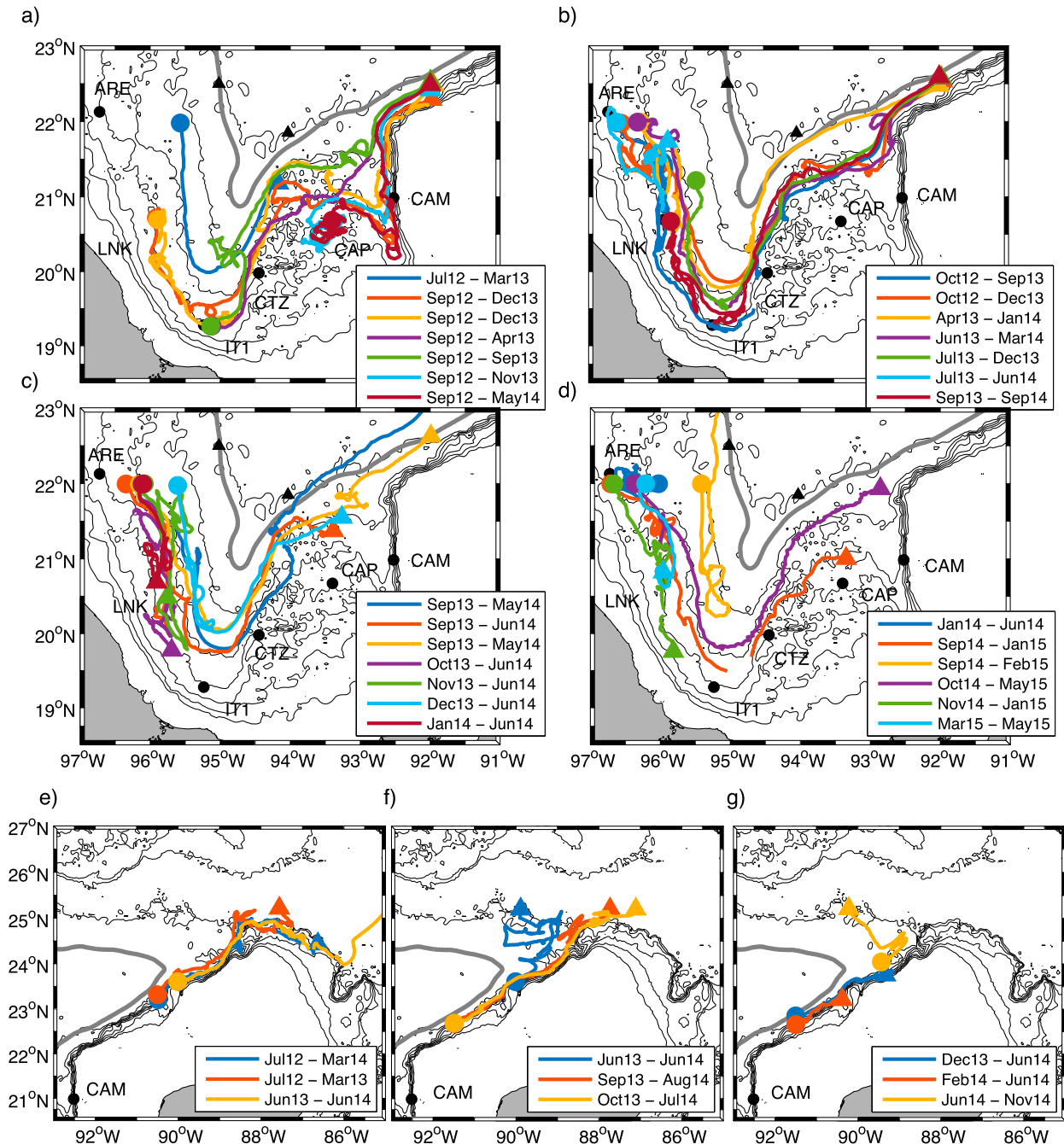


FIG. 11. As in Fig. 10, but for (a)–(d) Bay of Campeche continental slope and (e)–(g) Campeche Escarpment.

the westward translation of the anticyclonic eddies found at the point of separation is contributing significantly to the mean flow of the northern part of the SAG.

Note also that the highest EKE in the gyre is observed downstream of the point of separation, where the mean flow turns westward, and that relatively high EKE is observed along the northern part of the cyclonic gyre, while the western and southern limbs show a higher

contribution of the mean field, particularly where its flow converges with the boundary current off the western Campeche Escarpment (Figs. 5, 6). Hence, the deep mean flow in the abyssal plain is indeed a long-term average, and much variability is expected in the meso-scale range, as seen both from the EKE and independent float trajectories, particularly in the northern and western regions (Figs. 7c, 12b).

TABLE 3. Average transit times along western boundary, using float trajectories shown in Figs. 10 and 11.

Continental slope region (days)	Average transit time	No. of trajectories
Northwestern boundary (92°W to 23°N)	355	7
Western boundary (24°N to 21°N)	305	14
Bay of Campeche boundary (22°N to 92°W)	232	6
Campeche Escarpment (91.5°W to 88°W)	298	2

The SAG is located in a region that is rather flat, with low gradients of  $f/H$ , except near the Campeche Escarpment. This contrasts with the boundary flow, which is seen more clearly on top of regions with strong gradients of  $f/H$ . The fact that the gyre lies in the region of lowest  $f/H$  suggests that potential vorticity conservation is at play. The question remains as to what feeds the cyclonic vorticity. Since the gyre is located in a region of small slopes and low  $f/H$  gradients, only long-period TRWs could bring energy to the abyssal plain ( $T > 60$ – $100$  days; Oey and Lee 2002). Numerical results by Welsh and Inoue (2000) suggest that the cyclonic component of a modon traveling under a Loop Current ring survives longer in the western Gulf of Mexico and hence could result in a mean cyclonic flow in the abyssal plain. This seems confirmed by the analysis made with

the current meter mooring data used in Tenreiro et al. (2018).

The Loop Current eddies Icarus and Kraken were present in the abyssal plain between March 2012 and February 2013 and between August 2013 and February 2014, respectively (see Figs. 3-28 and 5-28 in Hamilton et al. 2016b). Between March and May 2014, an upper-layer anticyclone was found over the abyssal plain, but it is not clear if it was the remnant of Kraken or a locally formed eddy. The multimonth period of high tendency for cyclonic flow observed by the moorings after the passing of Icarus (February–April 2013) and Kraken (May–October 2014) coincides with a higher prevalence of cyclonic flow (Fig. 12). These assessments were made using the 17-cm sea surface height contour criteria (Leben 2005). The above eddy scenarios are consistent with cyclonic vorticity being brought to the region with the trailing edge of a modon traveling under the Loop Current eddies, and then remaining trapped in the low potential vorticity region after the surface eddy dissipated. Analogously, the reversals in the cyclonic tendency observed in October–November 2012 and May–September 2013 are consistent with the arrival of the leading edge anticyclone of these deep modons. Note that the moorings used in this study are the same as the ones used by Tenreiro et al. (2018), although the period analyzed is not exactly the same: they study Loop Current eddies present in the western basin between

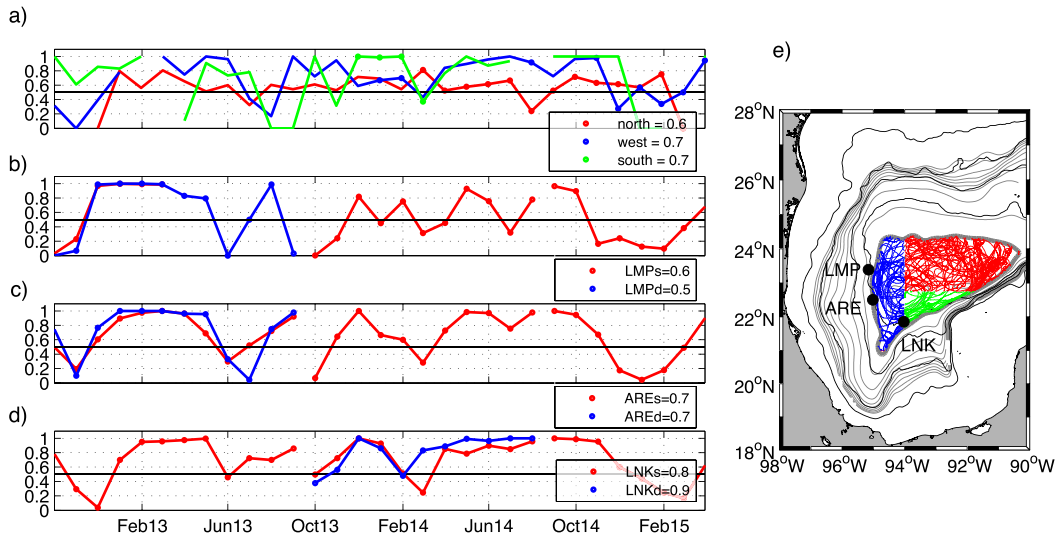


FIG. 12. Persistence of deep cyclonic gyre. (a) Time series of the fraction of smoothed float velocity observations at the deep cyclonic gyre in three regions: northern (red), western (blue), and southern (green) parts. Fewer than 100 observations were available at each time bin. (b)–(d) Monthly fraction of time with cyclonic flow at 1000 m (s; red) and 1500 m (d; blue) level for the moorings. The data at 1000 m were included given that there are large data gaps at 1500 m, and the currents at both depths show similar behavior. (e) Map showing locations of float velocity observations used and mooring positions. The  $f/H$  contours in gray as described in Fig. 4. Isobaths are shown as black contours at 1000, 2000, 3000, and 3500 m.

October 2008 and 2013, while the availability of float data in the abyssal plain occurs between October 2012 and June 2015 (Fig. 12).

Additional analysis of the float data shows that segments of their trajectories follow a dipolar circulation under Kraken (Furey et al. 2017, manuscript submitted to *J. Phys. Oceanogr.*), although no floats were able to make a full loop around coherent anticyclonic or cyclonic eddies in the deep basin (specifically, the region enclosed by the PV contour  $1.61 \times 10^{-8} \text{ m}^{-1} \text{ s}^{-1}$ ; see Fig. 4 for example), except for the anticyclones that appear at the point of separation in the Campeche Escarpment, which for the most part were seen after Kraken had passed through the region (Fig. 7c; Hamilton et al. 2016b). In addition, the longest flow reversal recorded by the moorings and floats in the western and southern gyre occurred between October 2014 and March 2015, a period of relative calm in the upper layer, since Kraken was the last LC eddy to enter the western basin during the period studied, and it had dissipated before then. Hence, conclusive evidence of modons traveling under Loop Current eddies is still lacking, and much remains to be understood of the contribution of LC eddies to the circulation in the abyssal plain.

A likely mechanism contributing to the mean cyclonic abyssal flow is eddy–topography interaction via bottom topographic form stresses (Holloway 1987; Cummins 1995; Thompson 1995, Dewar 1998; Hallberg and Rhines 2000). In particular, extensions of the Rhines and Young (1982) model to three layers with finite bottom topography show that the lower layer develops a cyclonic circulation in idealized basins with a continental slope, independently of the sign of the wind-driven circulation in the upper layer (Cummins 1995; Thompson 1995). This abyssal circulation is confined to the region of topographically closed geostrophic contours and is induced by bottom topographic form stresses that result from the momentum transferred to the bottom layer by an eddy potential vorticity flux. The latter represent the baroclinic instabilities of the upper-layer flow (Rhines and Young 1982), and hence a strong abyssal gyre depends on the closed  $f/H$  contours being near regions rich in baroclinic instabilities and eddies (Thompson 1995). Therefore, eddy–topography interaction is a likely mechanism to drive the SAG, given the relatively high EKE along the northern gyre and the presence of the eddies at the point of separation of the boundary flow on the Campeche Escarpment (Figs. 5, 7).

Low-frequency vortex stretching driven by low-frequency upwelling of the main thermocline over the abyssal plain, forced by the expansion of the LC in the eastern basin, may be another mechanism that could contribute to the modulation of the abyssal gyre, as has been suggested by Chang and Oey (2011).

Numerical models have reproduced the mean cyclonic circulation in the abyssal plain (e.g., Chang and Oey 2011; Bracco et al. 2016), and it is quite striking how the mean velocity field of the high-resolution model used in Bracco et al. (2016) also shows the SAG and boundary current as distinct features. The high mean velocities along the Campeche Escarpment and the separation of the boundary flow are both present in the model, although the separation occurs a bit farther east than what is observed by the floats. Therefore, these features appear to be real and persistent and not a result biased by the events observed by the float observations available nor the period analyzed.

#### 4. Conclusions and final remarks

A large dataset of subsurface floats parked at 1500 and 2500 m, covering the entire Gulf of Mexico between July 2011 and June 2015, has been analyzed. In addition, current meter moorings that were in place in the western GOM during this period are used to further understand the large-scale patterns of circulation in the deep layer of the GOM. The mean cyclonic circulation in the western GOM that has been suggested by previous numerical studies and patchy observational programs has been confirmed. The new finding is that the mean flow consists of two distinct features: a boundary current along the continental slope and a cyclonic gyre over the abyssal plain (Sigsbee Abyssal Gyre).

The dataset shows that the tendency for water to move cyclonically along the deep boundary current can last several months, but it is seen interrupted with periods of one to several months where both floats and moorings show a higher tendency for back-and-forth motion, and occasions with mean flow in the opposite direction. Independent float trajectories show back and forth motion or small-scale looping behavior embedded in a boundary flow, which in the majority of cases results in a net cyclonic displacement around the western Gulf of Mexico. Hence, the boundary flow allows water parcels to travel long distances around the gulf, with an estimated transit time of  $\sim 2$  years to move from the northern boundary (west of  $92^\circ\text{W}$ ) to the northwestern tip of the Campeche Bank (east of  $92^\circ\text{W}$ ). Although very few observations were at place along the northern slope of the Yucatan shelf–Campeche Bank, floats were shown to travel along this Escarpment into the eastern Gulf of Mexico.

One of the most remarkable findings of this experiment is the fact that part of the boundary current flow separates from the Campeche Escarpment at a fixed location near  $92^\circ\text{W}$ . This is quite striking since the separation occurs well downstream of the sharp turn of the

northwest corner of the Campeche Bank, which the floats (and boundary current) have no problem navigating. Of the floats that reached the Campeche Escarpment, ~30% continued east and the rest separated from the boundary. This process of separation was observed throughout the 1.5 years that floats were found flowing along the boundary current in the BOC, so we hypothesize it is a persistent feature that remains to be explained. Also noticeable is that more than 60% of the floats that separated from the boundary made at least one complete loop around deep anticyclones, and it is not clear if these eddies play a role in the separation process, or if the separation is involved in the genesis of these eddies, analogous to the process of formation of meddies (e.g., Bower et al. 1997; see also Furey et al. 2017, manuscript submitted to *J. Phys. Oceanogr.*).

The mean cyclonic circulation in the abyssal plain (SAG) is clearly bounded by topographically closed geostrophic contours, so eddy-topography interaction via bottom stress form drag is a likely mechanism to drive the gyre (e.g., Cummins 1995; Thompson 1995). Another contribution may be that cyclonic vorticity advected into the region by a dipole traveling under an LC eddy remains trapped in the low potential vorticity region of the abyssal plain when the LC eddy dissipates, as has been suggested by numerical experiments (Welsh and Inoue 2000) and observations (Tenreiro et al. 2018). No floats looped around coherent eddies in the abyssal plain, except for the anticyclones that appear in the region of separation of the boundary flow (Fig. 7c), but a more detailed analysis by Furey et al. (2017, manuscript submitted to *J. Phys. Oceanogr.*) shows segments of the float trajectories following a dipolar circulation under Kraken in the western basin, so it may well be that these modons do exist. Nevertheless, both the moorings and float data show indications of low-frequency variability in the SAG flow in a period when no LC eddies were present in the region, so much remains to be understood on the processes involved in sustaining the mean angular momentum in the deep basin, and the role that LC eddies play in the SAG's existence and variability.

The float dataset is unprecedented in its regional scope and long record, and it has shown a rather continuous pathway for tracers to be advected around the western basin. Ongoing analysis combining altimetry with the float trajectories is giving quite a bit of insight on the stirring that occurs in the lower layer as a result of the Loop Current dynamics in the eastern Gulf and the interaction of LC eddies Icarus and Kraken with the northern and western continental slopes (see preliminary results in Hamilton et al. 2016b). The period when Kraken was present is the best sampled by the floats in the western basin; hence, an in-depth analysis of the influence this LC eddy had in the lower layer merits further attention, particularly given that this energetic ring remained largely coherent until it started interacting with the western

boundary (J. Olascoaga et al. 2017, unpublished manuscript). A first look into the interaction of Kraken with the lower layer, its relation to the intensification of the SAG and boundary current flow, and possible contribution to the formation of deep eddies off Campeche Escarpment is explored with the same float dataset in Furey et al. (2017, manuscript submitted to *J. Phys. Oceanogr.*).

*Acknowledgments.* This work was supported by the Bureau of Ocean Energy Management (BOEM) under Contract M10PC00112 assigned to Leidos, Inc. Original float data are available at the NOAA/AOML subsurface float observations archive ([http://www.aoml.noaa.gov/phod/float\\_traj/index.php](http://www.aoml.noaa.gov/phod/float_traj/index.php)), and the gridded float data statistics are available at the BOEM data archive, thanks to the help of Jonathan Blythe ([https://opendata.boem.gov/GriddedFields\\_1500m\\_floats\\_CF.nc](https://opendata.boem.gov/GriddedFields_1500m_floats_CF.nc)). We are very grateful to Alexis Lugo-Fernández (BOEM) for his support and involvement in the planning, execution, and discussion of the results of the float program from its onset until its end. Julio Sheinbaum (CICESE) provided valuable insights and literature. Sound source mooring installation and recovery as well as float deployments were completed successfully thanks to the support of Jim Singer (Leidos, Inc.), Brian Guest (WHOI), the Canek group (CICESE), and the crews of the R/V *Pelican* (LUMCON) and B/O *Justo Sierra* (UNAM). ADCP mooring data were part of the CICESE-Petróleos Mexicanos Grant PEP-CICESE 428229851. We extend our thanks to the Canek group and the crew of the B/O *Justo Sierra* for ADCP mooring installation, recovery, data acquisition, and processing. We appreciate the kind comments from two reviewers that helped make this manuscript clearer.

## REFERENCES

- Biggs, D. C., G. S. Fargion, P. Hamilton, and R. R. Leben, 1996: Cleavage of a Gulf of Mexico Loop Current eddy by a deep water cyclone. *J. Geophys. Res.*, **101**, 20 629–20 641, <https://doi.org/10.1029/96JC01078>.
- Bower, A. S., L. Armi, and I. Ambar, 1997: Lagrangian observations of meddy formation during a Mediterranean undercurrent seeding experiment. *J. Phys. Oceanogr.*, **27**, 2545–2575, [https://doi.org/10.1175/1520-0485\(1997\)027<2545:LOOMFD>2.0.CO;2](https://doi.org/10.1175/1520-0485(1997)027<2545:LOOMFD>2.0.CO;2).
- Bracco, A., J. Choi, K. Joshi, H. Luo, and J. C. McWilliams, 2016: Submesoscale currents in the Northern Gulf of Mexico: Deep phenomena and dispersion over the continental slope. *Ocean Modell.*, **101**, 43–58, <https://doi.org/10.1016/j.ocemod.2016.03.002>.
- Candela, J., J. Sheinbaum, J. Ochoa, A. Badan, and R. Leben, 2002: The potential vorticity flux through the Yucatan Channel and the Loop Current in the Gulf of Mexico. *Geophys. Res. Lett.*, **29**, 2059, <https://doi.org/10.1029/2002GL015587>.
- Chang, Y. L., and L.-Y. Oey, 2011: Loop current cycle: Coupled response of the Loop Current with deep flows. *J. Phys. Oceanogr.*, **41**, 458–471, <https://doi.org/10.1175/2010JPO4479.1>.
- Cummins, P. F., 1995: Relative angular momentum balances of quasi-geostrophic circulation models. *J. Mar. Res.*, **53**, 315–340, <https://doi.org/10.1357/0022240953213160>.

- DeHaan, C. J., and W. Sturges, 2005: Deep cyclonic circulation in the Gulf of Mexico. *J. Phys. Oceanogr.*, **35**, 1801–1812, <https://doi.org/10.1175/JPO2790.1>.
- Dewar, W. K., 1998: Topography and barotropic transport control by bottom friction. *J. Mar. Res.*, **56**, 295–328, <https://doi.org/10.1357/002224098321822320>.
- Donohue, K. A., P. Hamilton, K. Leaman, R. Leben, M. Prater, D. R. Watts, and E. Waddell, 2006: Exploratory study of deepwater currents in the Gulf of Mexico: Volume II: Technical report. OCS Study MMS 2006-074, 408 pp., <https://www.boem.gov/ESPIS/4/4222.pdf>.
- , D. R. Watts, P. Hamilton, R. Leben, and M. Kennelly, 2016: Loop Current eddy formation and baroclinic instability. *Dyn. Atmos. Oceans*, **76**, 195–216, <https://doi.org/10.1016/j.dynatmoce.2016.01.004>.
- Emery, W. J., and R. E. Thomson, 2001: *Data Analysis Methods in Physical Oceanography*. 2nd ed. Elsevier Science, 654 pp.
- Hall, C. A., and R. R. Leben, 2016: Observational evidence of seasonality in the timing of Loop Current eddy separation. *Dyn. Atmos. Oceans*, **76**, 240–267, <https://doi.org/10.1016/j.dynatmoce.2016.06.002>.
- Hallberg, R., and P. B. Rhines, 2000: Boundary sources of potential vorticity in geophysical circulations. *Developments in Geophysical Turbulence*, R. M. Kerr and Y. Kimura, Eds., Kluwer, 51–65.
- Hamilton, P., 1990: Deep currents in the Gulf of Mexico. *J. Phys. Oceanogr.*, **20**, 1087–1104, [https://doi.org/10.1175/1520-0485\(1990\)020<1087:DCITGO>2.0.CO;2](https://doi.org/10.1175/1520-0485(1990)020<1087:DCITGO>2.0.CO;2).
- , 2002: On the structure and motions of cyclones in the northern Gulf of Mexico. *J. Geophys. Res.*, **107**, 3208, <https://doi.org/10.1029/1999JC000270>.
- , 2009: Topographic Rossby waves in the Gulf of Mexico. *Prog. Oceanogr.*, **82**, 1–31, <https://doi.org/10.1016/j.pocean.2009.04.019>.
- , and A. Lugo Fernandez, 2001: Observations of high speed deep currents in the northern Gulf of Mexico. *Geophys. Res. Lett.*, **28**, 2867–2870, <https://doi.org/10.1029/2001GL013039>.
- , K. Donohue, C. Hall, R. R. Leben, H. Quian, J. Sheinbaum, and D. R. Watts, 2015: Observations and dynamics of the Loop Current. OCS Study BOEM 2015-006, 417 pp., <https://www.boem.gov/ESPIS/5/5471.pdf>.
- , A. Lugo-Fernández, and J. Sheinbaum, 2016a: A Loop Current experiment: Field and remote measurements. *Dyn. Atmos. Oceans*, **76**, 156–173, <https://doi.org/10.1016/j.dynatmoce.2016.01.005>.
- , A. Bower, H. Furey, R. R. Leben, and P. Pérez-Brunius, 2016b: Deep circulation in the Gulf of Mexico: A Lagrangian study. OCS Study BOEM 2016-081, 289 pp., <https://www.boem.gov/ESPIS/5/5583.pdf>.
- Hofmann, E. E., and S. J. Worley, 1986: An investigation of the circulation of the Gulf of Mexico. *J. Geophys. Res.*, **91**, 14 221–14 236, <https://doi.org/10.1029/JC091iC12p14221>.
- Holloway, G., 1987: Systematic forcing of large-scale geophysical flows by eddy-topography interaction. *J. Fluid Mech.*, **184**, 463–476, <https://doi.org/10.1017/S0022112087002970>.
- Hurlburt, H. E., and J. D. Thompson, 1980: A numerical study of Loop Current intrusions and eddy shedding. *J. Phys. Oceanogr.*, **10**, 1611–1651, [https://doi.org/10.1175/1520-0485\(1980\)010<1611:ANSOLC>2.0.CO;2](https://doi.org/10.1175/1520-0485(1980)010<1611:ANSOLC>2.0.CO;2).
- , and —, 1982: The dynamics of the Loop Current and shed eddies in a numerical model of the Gulf of Mexico. *Hydrodynamics of Semi-Enclosed Seas*, Elsevier Oceanography Series, Vol. 34, Elsevier, 243–297, [https://doi.org/10.1016/S0422-9894\(08\)71247-9](https://doi.org/10.1016/S0422-9894(08)71247-9).
- Jouanno, J., J. Ochoa, E. Pallàs-Sanz, J. Sheinbaum, F. Andrade-Canto, J. Candela, and J.-M. Molines, 2016: Loop Current frontal eddies: Formation along the Campeche Bank and impact of coastally trapped waves. *J. Phys. Oceanogr.*, **46**, 3339–3363, <https://doi.org/10.1175/JPO-D-16-0052.1>.
- Kolodziejczyk, N., J. Ochoa, J. Candela, and J. Sheinbaum, 2011: Deep currents in the Bay of Campeche. *J. Phys. Oceanogr.*, **41**, 1902–1920, <https://doi.org/10.1175/2011JPO4526.1>.
- LaCasce, J. H., 1998: A geostrophic vortex over a slope. *J. Phys. Oceanogr.*, **28**, 2362–2381, [https://doi.org/10.1175/1520-0485\(1998\)028<2362:AGVOAS>2.0.CO;2](https://doi.org/10.1175/1520-0485(1998)028<2362:AGVOAS>2.0.CO;2).
- , 2008: Statistics from Lagrangian observations. *Prog. Oceanogr.*, **77**, 1–29, <https://doi.org/10.1016/j.pocean.2008.02.002>.
- Leben, R. R., 2005: Altimeter-derived Loop Current metrics. *Circulation in the Gulf of Mexico*, *Geophys. Monogr.*, Vol. 161, Amer. Geophys. Union, 181–201, <https://doi.org/10.1029/161GM15>.
- Lee, H.-C., 2003: Numerical simulation of the Gulf Stream System: The Loop Current and the deep circulation. *J. Geophys. Res.*, **108**, 3043, <https://doi.org/10.1029/2001JC001074>.
- Lilly, J. M., 2017: jLab: A data analysis package for Matlab, version 1.6.3. Accessed 10 January 2018, <http://www.jmlilly.net/jmlsoft.html>.
- Mahadevan, A., L. N. Thomas, and A. Tandon, 2008: Comment on “Eddy/wind interactions stimulate extraordinary mid-ocean plankton blooms.” *Science*, **320**, 448, <https://doi.org/10.1126/science.1152111>.
- Martin, R. G., and A. H. Bouma, 1978: Physiography of Gulf of Mexico. *Framework, Facies, and Oil Trapping Characteristics of the Upper Continental Margin*, A. H. Bouma, G. T. Moore, and J. M. Coleman, Eds., AAPG Studies in Geology, Vol. 7, American Association of Petroleum Geologists, 3–19.
- Mizuta, G., and N. G. Hogg, 2004: Structure of the circulation induced by a shoaling topographic wave. *J. Phys. Oceanogr.*, **34**, 1793–1810, [https://doi.org/10.1175/1520-0485\(2004\)034<1793:SOTCIB>2.0.CO;2](https://doi.org/10.1175/1520-0485(2004)034<1793:SOTCIB>2.0.CO;2).
- NOAA, 2017: History of NOAA ocean exploration: Timeline. Accessed 5 July 2017, <http://oceanexplorer.noaa.gov/history/timeline/timeline.html>.
- Oey, L.-Y., 2008: Loop Current and deep eddies. *J. Phys. Oceanogr.*, **38**, 1426–1449, <https://doi.org/10.1175/2007JPO3818.1>.
- , and H.-C. Lee, 2002: Deep eddy energy and topographic Rossby waves in the Gulf of Mexico. *J. Phys. Oceanogr.*, **32**, 3499–3527, [https://doi.org/10.1175/1520-0485\(2002\)032<3499:DEEATR>2.0.CO;2](https://doi.org/10.1175/1520-0485(2002)032<3499:DEEATR>2.0.CO;2).
- , T. Ezer, and H.-C. Lee, 2005: Loop Current, rings and related circulation in the Gulf of Mexico: A review of numerical models and future challenges. *Circulation in the Gulf of Mexico: Observations and Models*, *Geophys. Monogr.*, Vol. 161, Amer. Geophys. Union, 31–56, <https://doi.org/10.1029/161GM04>.
- Pérez-Brunius, P., P. García-Carrillo, J. Dubranna, J. Sheinbaum, and J. Candela, 2013: Direct observations of the upper layer circulation in the southern Gulf of Mexico. *Deep-Sea Res. II*, **85**, 182–194, <https://doi.org/10.1016/j.dsr2.2012.07.020>.
- Rhines, P. B., and W. R. Young, 1982: A theory of the wind-driven circulation I. Mid-ocean gyres. *J. Mar. Res.*, **40**, 559–596.
- Rossby, T., D. Dorson, and J. Fontaine, 1986: The RAFOS system. *J. Atmos. Oceanic Technol.*, **3**, 672–679, [https://doi.org/10.1175/1520-0426\(1986\)003<0672:TRS>2.0.CO;2](https://doi.org/10.1175/1520-0426(1986)003<0672:TRS>2.0.CO;2).
- Sheinbaum, J., J. Ochoa, J. Candela, and A. Badan, 2010: Full-water column current observations in the western Gulf of Mexico. OCS Study BOEMRE 2010-044, 108 pp., <https://www.boem.gov/ESPIS/4/5093.pdf>.

- , G. Athié, J. Candela, J. Ochoa, and A. Romero-Arteaga, 2016: Structure and variability of the Yucatan and Loop Currents along the slope and shelf break of the Yucatan Channel and Campeche Bank. *Dyn. Atmos. Oceans*, **76**, 217–239, <https://doi.org/10.1016/j.dynatmoce.2016.08.001>.
- Sturges, W., J. C. Evans, and S. Welsh, 1993: Separation of warm-core rings in the Gulf of Mexico. *J. Phys. Oceanogr.*, **23**, 250–268, [https://doi.org/10.1175/1520-0485\(1993\)023<0250:SOWCRI>2.0.CO;2](https://doi.org/10.1175/1520-0485(1993)023<0250:SOWCRI>2.0.CO;2).
- Tenreiro, M., J. Candela, E. Pallàs-Sanz, J. Sheinbaum, and J. Ochoa, 2018: Near surface and deep circulation coupling in the western Gulf of Mexico. *J. Phys. Oceanogr.*, **48**, 145–161, <https://doi.org/10.1175/JPO-D-17-0018.1>.
- Thompson, L., 1995: The effect of continental rises on the wind-driven ocean circulation. *J. Phys. Oceanogr.*, **25**, 1296–1316, [https://doi.org/10.1175/1520-0485\(1995\)025<1296:TEOCRO>2.0.CO;2](https://doi.org/10.1175/1520-0485(1995)025<1296:TEOCRO>2.0.CO;2).
- Vidal, V. M. V., F. V. Vidal, and J. M. Pérez-Molero, 1992: Collision of a Loop Current anticyclonic ring against the continental shelf slope of the western Gulf of Mexico. *J. Geophys. Res.*, **97**, 2155–2172, <https://doi.org/10.1029/91JC00486>.
- , —, A. F. Hernández, E. Meza, and L. Zambrano, 1994: Winter water mass distributions in the western Gulf of Mexico affected by a colliding anticyclonic ring. *J. Oceanogr.*, **50**, 559–588, <https://doi.org/10.1007/BF02235424>.
- Weatherly, G. L., N. Wienders, and A. Romanou, 2005: Intermediate-depth circulation in the Gulf of Mexico estimated from direct measurements. *Circulation in the Gulf of Mexico: Observations and Models*, *Geophys. Monogr.*, Vol. 161, Amer. Geophys. Union, 315–324, <https://doi.org/10.1029/161GM22>.
- Welsh, S. E., and M. Inoue, 2000: Loop Current rings and the deep circulation in the Gulf of Mexico. *J. Geophys. Res.*, **105**, 16 951–16 959, <https://doi.org/10.1029/2000JC900054>.